

Mass Spectra of Heavy-Light Mesons in Heavy Hadron Chiral Perturbation Theory

Mohammad H. Alhakami

Nuclear Science Research Institute

KACST, P.O. Box 6086, Riyadh 11442, Saudi Arabia

(Dated: July 14, 2016)

We study the masses of the low-lying charm and bottom mesons within the framework of heavy hadron chiral perturbation theory (HHChPT). We work to third order in the chiral expansion, where meson loops contribute. In contrast to previous approaches, we use physical meson masses in evaluating these loops. This ensures that their imaginary parts are consistent with the observed widths of the D -mesons. The lowest odd- and even-parity, strange and nonstrange charm mesons provide enough constraints to determine only certain linear combinations of the low-energy constants in the effective Lagrangian. We comment on how lattice QCD could provide further information to disentangle these constants. Then we use the results from the charm sector to predict the spectrum of odd- and even-parity of the bottom mesons. The predicted masses from our theory are in good agreement with experimentally measured masses for the case of the odd-parity sector. For the even-parity sector, the B -meson states have not yet been observed; thus, our results provide useful information for experimentalists investigating such states. The near degeneracy of nonstrange and strange scalar B mesons is confirmed in our predictions using HHChPT. We show why previous approaches of using HHChPT in studying the mass degeneracy in the scalar states of charm and bottom meson sectors gave unsatisfactory results.

I. INTRODUCTION

The masses and widths of the low-lying charm mesons are now rather well determined experimentally, in the odd- and even-parity, strange and nonstrange sectors (for summaries, see Refs. [1, 2]). The patterns of the masses and interactions of these mesons are governed by two approximate symmetries: the spin symmetry of the heavy quark and the $SU(3)_L \times SU(3)_R$ chiral symmetry of the light quarks. Both symmetries can be incorporated in a single framework using heavy-hadron chiral perturbation theory (HHChPT), an effective field theory for the interactions of a meson containing a single heavy quark [3–8].

Within this theory, the masses of the low-lying odd- and even-parity D mesons have been studied, including one-loop chiral corrections [9, 10]. The chiral Lagrangian at this, third, order contains a number of unknown low-energy constants (LECs). These cannot be determined uniquely from experimental data on the meson spectrum because their number exceeds the number of low-lying mesons. Mehen and Springer [9] and Ananthanarayan *et al.* [10] fitted expressions that depend nonlinearly on these constants and found multiple solutions, often with quite different numerical values for them. As a result, no clear pattern emerged from these fits.

In this paper, we use a different approach to fit these parameters to remove these ambiguities and provide a clearer picture. The key difference from previous work [9, 10] is that we use the physical values of the charm meson masses in evaluating the chiral loops. One important consequence of this is to put thresholds at the correct energies relative to the masses of unstable particles and hence to ensure that the imaginary parts of the loops are correctly related to the observed decay widths of the heavy mesons. A second consequence is that the parameters – the LECs – appear only in the tree-level contributions to the masses. This allows us to determine uniquely eight linear combinations of the LECs from the experimental masses. These eight parameters cannot be further disentangled into the individual LECs using the experimental spectrum alone. By using the experimental masses in the loops, we generate terms that are of order higher than third order in the chiral expansion. These include divergences that we cannot cancel using counterterms in our Lagrangian. We use the β -functions associated with these uncontrolled higher-order contributions to provide an estimate of the theoretical errors introduced by our approach. Another, more technical, difference from previous work on HHChPT is that we have used corrected expressions for the chiral loop functions, in contrast to the expressions presented in [7, 9] which use an inconsistent renormalization scheme.

The results from the charm meson sector are used to predict the masses of the full set of the low-lying B -meson states. The predicted masses from our theory of the ground states are in good agreement with the well-determined masses. The first set of excited B meson states has not yet been observed; thus our results can be used to provide useful information for experimentalists investigating such states. The near degeneracy of scalar B meson states – the mass of the nonstrange scalar B -meson is similar to that of strange one – is confirmed in our predictions using HHChPT. Our results are at variance with those in Ref. [11]. We will show why the previous studies of the near mass degeneracy in the scalar D - and B -meson sectors using the approach of HHChPT led to unsatisfactory results.

This paper is organized as follows. In Sec. II, the heavy-hadron chiral Lagrangian we use is briefly reviewed. In Sec. III, we present the resulting expression for the meson masses. Since the number of the LECs exceeds the number of observables, the LECs are grouped into eight linear combinations that are equivalent to the number of observables. In Sec. IV, we use the D -meson spectrum to fit these parameters. The results from the charm meson spectrum are then used in Sec. V to predict the masses of the low-lying bottom meson states. The summary is given in Sec. VI.

II. HEAVY-HADRON CHIRAL LAGRANGIAN

Our starting point is the same effective Lagrangian that was used in Refs. [9, 10]. We give a brief outline of it here; more details can be found in those papers and the review by Casalbuoni *et al.* [7]. In the heavy quark limit, systems with a single heavy quark respect heavy-quark spin symmetry, forming degenerate multiplets independent of the spin orientation of the quark. The lowest multiplet of charm mesons consists of the pseudoscalar ground states, D^0 , D^+ and D_s^+ , and their vector first excited states, D^{*0} , D^{*+} and D_s^{*+} . These can be conveniently described by the effective field,

$$\mathcal{H}_a = \frac{1 + \not{v}}{2} (H_a^\mu \gamma_\mu - H_a \gamma_5), \quad (1)$$

where the fields H_a annihilate the pseudoscalar particles and H_a^μ annihilate the vector ones. Here, the flavor index $a = 1, 2, 3$ denotes states with up, down, and strange quarks, respectively. The first excited multiplet has the opposite parity and consists of scalar, D_0^0 , D_0^+ and D_{0s}^+ , and axial-vector mesons, $D_1^{0'}$, $D_1^{1'}$ and $D_{1s}^{0'}$. These can be described by the effective field,

$$\mathcal{S}_a = \frac{1 + \not{v}}{2} (S_a^\mu \gamma_\mu \gamma_5 - S_a), \quad (2)$$

where the fields S_a and S_a^μ annihilate the scalar and axial-vector particles, respectively.

The other ingredient of the theory is the approximate $SU(3)_L \times SU(3)_R$ chiral symmetry of QCD. This is embodied by fields describing the lightest strongly interacting particles, π , K and η , which are approximately the Goldstone bosons of this hidden symmetry. These can be represented by the matrix field $U(x) = \exp(i\sqrt{2}\phi(x)/f)$ where $\phi(x)$ is given by

$$\phi(x) = \begin{pmatrix} \frac{1}{\sqrt{2}}\pi^0 + \frac{1}{\sqrt{6}}\eta & \pi^+ & K^+ \\ \pi^- & -\frac{1}{\sqrt{2}}\pi^0 + \frac{1}{\sqrt{6}}\eta & K^0 \\ K^- & \bar{K}^0 & -\sqrt{\frac{2}{3}}\eta \end{pmatrix}. \quad (3)$$

In our conventions, we use the physical value of the pion decay constant $f = 92.4$ MeV. It is different from the ones used by Wise in [3] in which $f = 135$ MeV was used. Thus, one has to replace f in [3] by $\sqrt{2}f$ to account for different conventions. The lowest-order Lagrangian for the light mesons is

$$\mathcal{L}_m = \frac{f^2}{4} \text{Tr} (\partial_\mu U \partial^\mu U^\dagger) + \frac{f^2 B_0}{2} \text{Tr} (m_q U^\dagger + U m_q^\dagger), \quad (4)$$

where the coefficient B_0 is related to the pion decay constant and the quark condensate of light quark flavors [12]. The light quark mass matrix is given by $m_q = \text{diag}(m_u, m_d, m_s)$.

We take as our low-energy scales, generically denoted by Q , the masses and momenta of the Goldstone bosons and the splittings between the four lowest states of the D mesons introduced above. The relevant expression of the heavy-hadron chiral Lagrangian up to order Q^3 is [4, 9]

$$\begin{aligned} \mathcal{L}_H = & -\text{Tr}[\bar{\mathcal{H}}_a (iv \cdot D_{ba} - \delta_H \delta_{ab}) \mathcal{H}_b] + \text{Tr}[\bar{\mathcal{S}}_a (iv \cdot D_{ba} - \delta_S \delta_{ab}) \mathcal{S}_b] \\ & + g \text{Tr}[\bar{\mathcal{H}}_a \mathcal{H}_b \not{u}_{ba} \gamma_5] + g' \text{Tr}[\bar{\mathcal{S}}_a \mathcal{S}_b \not{u}_{ba} \gamma_5] + h \text{Tr}[\bar{\mathcal{H}}_a \mathcal{S}_b \not{u}_{ba} \gamma_5 + \text{h.c.}] \\ & - \frac{\Delta_H}{8} \text{Tr}[\bar{\mathcal{H}}_a \sigma^{\mu\nu} \mathcal{H}_a \sigma_{\mu\nu}] + \frac{\Delta_S}{8} \text{Tr}[\bar{\mathcal{S}}_a \sigma^{\mu\nu} \mathcal{S}_a \sigma_{\mu\nu}] \\ & + a_H \text{Tr}[\bar{\mathcal{H}}_a \mathcal{H}_b] m_{ba}^\xi - a_S \text{Tr}[\bar{\mathcal{S}}_a \mathcal{S}_b] m_{ba}^\xi + \sigma_H \text{Tr}[\bar{\mathcal{H}}_a \mathcal{H}_a] m_{bb}^\xi - \sigma_S \text{Tr}[\bar{\mathcal{S}}_a \mathcal{S}_a] m_{bb}^\xi \\ & - \frac{\Delta_H^{(a)}}{8} \text{Tr}[\bar{\mathcal{H}}_a \sigma^{\mu\nu} \mathcal{H}_b \sigma_{\mu\nu}] m_{ba}^\xi + \frac{\Delta_S^{(a)}}{8} \text{Tr}[\bar{\mathcal{S}}_a \sigma^{\mu\nu} \mathcal{S}_b \sigma_{\mu\nu}] m_{ba}^\xi \\ & - \frac{\Delta_H^{(\sigma)}}{8} \text{Tr}[\bar{\mathcal{H}}_a \sigma^{\mu\nu} \mathcal{H}_a \sigma_{\mu\nu}] m_{bb}^\xi + \frac{\Delta_S^{(\sigma)}}{8} \text{Tr}[\bar{\mathcal{S}}_a \sigma^{\mu\nu} \mathcal{S}_a \sigma_{\mu\nu}] m_{bb}^\xi, \end{aligned} \quad (5)$$

where the covariant derivative is defined as $D_{ba}^\mu = \partial_{ba}^\mu + \frac{1}{2}(\xi^\dagger \partial^\mu \xi + \xi \partial^\mu \xi^\dagger)_{ba}$, $\xi(x) = \sqrt{U(x)}$. The factors δ_H and δ_S are the residual masses of the effective fields \mathcal{H}_a and \mathcal{S}_a , respectively. The coupling constant g (g') measures the strength of transitions within odd- (even-)parity charm meson states. The strength of transitions between odd- and even-parity states is measured by the coupling constant h . The axial vector field is $u_{ba}^\mu = \frac{i}{2}(\xi^\dagger \partial^\mu \xi - \xi \partial^\mu \xi^\dagger)_{ba}$. The hyperfine splittings of the D -meson states are measured by $(\Delta, \Delta^{(a)}, \Delta^{(\sigma)})$. These coefficients manifestly vanish in the heavy quark limit. The quark mass matrix which breaks chiral symmetry is defined as $m_{ba}^\xi = \frac{1}{2}(\xi m_q \xi + \xi^\dagger m_q \xi^\dagger)_{ba}$. The coefficients (a, σ) present in the chirally breaking terms are dimensionless.

According to our power counting, the terms in the first three lines in Eq. (5) are all of order Q^1 . These include terms, in the third line, that break the heavy-quark spin symmetry. Since, at leading order, the quark masses are proportional to the squares of the masses of the Goldstone bosons, the chiral-symmetry breaking terms in the fourth line are of order Q^2 . The final terms which break both chiral and heavy-quark spin symmetries are of order Q^3 . These terms are required to cancel the infinite parts resulting from regularization and renormalization of the loop diagrams, note that all diagrams are of order Q^3 .

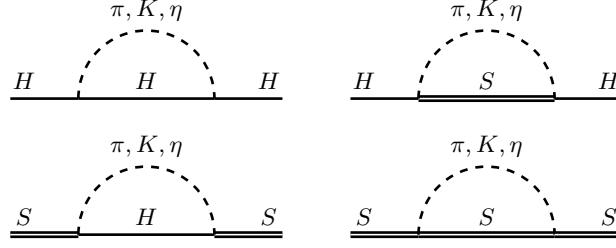


FIG. 1. The self-energy diagrams for the ground-state fields H and the excited-state fields S .

III. MASS FORMULA OF THE CHARM MESONS

The full contributions to the physical mass can be obtained by adding the tree-level contributions to the one-loop corrections $\Sigma_{D^{(*)}}$ as

$$\begin{aligned}
 m_{H_a} &= \delta_H + a_H m_a + \sigma_H \bar{m} - \frac{3}{4}(\Delta_H + \Delta_H^{(a)} m_a + \Delta_H^{(\sigma)} \bar{m}) + \Sigma_{H_a}, \\
 m_{H_a^*} &= \delta_H + a_H m_a + \sigma_H \bar{m} + \frac{1}{4}(\Delta_H + \Delta_H^{(a)} m_a + \Delta_H^{(\sigma)} \bar{m}) + \Sigma_{H_a^*}, \\
 m_{S_a} &= \delta_S + a_S m_a + \sigma_S \bar{m} - \frac{3}{4}(\Delta_S + \Delta_S^{(a)} m_a + \Delta_S^{(\sigma)} \bar{m}) + \Sigma_{S_a}, \\
 m_{S_a^*} &= \delta_S + a_S m_a + \sigma_S \bar{m} + \frac{1}{4}(\Delta_S + \Delta_S^{(a)} m_a + \Delta_S^{(\sigma)} \bar{m}) + \Sigma_{S_a^*},
 \end{aligned} \tag{6}$$

where we use the notation of Ref. [9]. Here, we work in the isospin limit ($m_u = m_d = m_1$) where $\bar{m} = 2m_1 + m_3$ and $m_a = (m_1, m_1, m_3)$. The Feynman diagrams of the one-loop corrections $\Sigma_{D^{(*)}}$ to the masses of D -mesons are shown in Fig.1. The resulting explicit expressions for the self energies of the charm mesons are given in Appendix A. In our work, the residual masses $m_{D^{(*)}}$ are measured from the nonstrange spin-averaged H mass, $(m_{H_1} + 3m_{H_1^*})/4$.

The existing coefficients in Eq. (6) can be either determined from experiments or from lattice fit. In Refs. [9, 10], the authors fitted the above expressions which depend nonlinearly on these coefficients and found multiple solutions, often with quite different numerical values for them. As a result, no clear pattern emerged from these fits. This is because the number of these coefficients exceeds the number of experimentally known charm meson masses. Thus, getting unique numerical values of the coefficients is impossible. Here, we attempt to remove this ambiguity by following a different approach to fit these coefficients. We use the physical values of the masses in evaluating the chiral loops. As a consequence, the energy of any unstable particle is placed correctly relative to the decay threshold, and the imaginary part of the loop integral can be related to the experimental decay width. The second effect is to reduce the number of unknown coefficients in comparison with the current experimental data on charm meson masses. Masses at tree level depend only on certain linear combinations of LECs. By using physical masses in chiral loops, the masses still depend linearly on these combinations. Therefore, one can express these combination of LECs directly in terms of the physical masses and loop integrals.

The procedure of combining the LECs is performed according to the symmetry patterns of the charm mesons. In this manner, the constructed parameters can be uniquely determined by using available experimental values of the meson masses and widths. The parameters that respect flavor symmetry are

$$\begin{aligned}
 \eta_H &= \delta_H + \left(\frac{a_H}{3} + \sigma_H\right) \bar{m}, \quad \xi_H = \Delta_H + \left(\frac{\Delta_H^{(a)}}{3} + \Delta_H^{(\sigma)}\right) \bar{m}, \\
 \eta_S &= \delta_S + \left(\frac{a_S}{3} + \sigma_S\right) \bar{m}, \quad \xi_S = \Delta_S + \left(\frac{\Delta_S^{(a)}}{3} + \Delta_S^{(\sigma)}\right) \bar{m},
 \end{aligned} \tag{7}$$

where $\delta_{H;S}$ and $\Delta_{H;S}$ respect chiral symmetry, but the other terms contain the average of the quark masses \bar{m} which

breaks it. The parameters left after constructing η_H , η_S , ξ_H , and ξ_S are

$$\begin{aligned} L_H &= (m_3 - m_1) a_H, \quad T_H = (m_3 - m_1) \Delta_H^{(a)}, \\ L_S &= (m_3 - m_1) a_S, \quad T_S = (m_3 - m_1) \Delta_S^{(a)}. \end{aligned} \quad (8)$$

The combinations $L_{H;S}$ and $T_{H;S}$ break flavor symmetry, and the latter also breaks spin symmetry. In terms of these linear combinations, the masses can be written as

$$\begin{aligned} m_{H_a} &= \eta_H - \frac{3}{4}\xi_H + \frac{\alpha_a}{3}L_H + \frac{\beta_a}{2}T_H + \Sigma_{H_a}, \\ m_{H_a^*} &= \eta_H + \frac{1}{4}\xi_H + \frac{\alpha_a}{3}L_H + \frac{\beta_a^*}{2}T_H + \Sigma_{H_a^*}, \\ m_{S_a} &= \eta_S - \frac{3}{4}\xi_S + \frac{\alpha_a}{3}L_S + \frac{\beta_a}{2}T_S + \Sigma_{S_a}, \\ m_{S_a^*} &= \eta_S + \frac{1}{4}\xi_S + \frac{\alpha_a}{3}L_S + \frac{\beta_a^*}{2}T_S + \Sigma_{S_a^*}, \end{aligned} \quad (9)$$

where α_a and $\beta_a^{(*)}$ are $\alpha_1 = -1$, $\alpha_3 = 2$, $\beta_1 = 1/2$, $\beta_3 = -1$, $\beta_1^* = -1/6$, and $\beta_3^* = 1/3$. Now, the number of parameters, $\xi_{H;S}$, $\eta_{H;S}$, $L_{H;S}$, and $T_{H;S}$ is 8, which is equal to the number of observed low-lying D -meson states.

IV. DETERMINATION OF LOW-ENERGY CONSTANTS

The numerical values of the parameters ($\xi_{H;S}$, $\eta_{H;S}$, $L_{H;S}$, $T_{H;S}$) will be given in this part. In our fitting, the physical masses and the coupling constants extracted from the well-measured widths are used. The used meson masses are two masses of the ground-state nonstrange mesons in the isospin limit and four masses of strange mesons from both sectors, see Table I. The excited nonstrange mesons are reported with the large uncertainties. In this case, we did not take the isospin average and instead the masses of the neutral heavy mesons ($m_{D_0^0} = 2318 \pm 29$ MeV [1], $m_{D_1^{0'}} = 2427 \pm 36$ MeV [13]) are chosen due to their relatively small errors in comparison with the excited charged mesons [1, 13–18]. The masses of the Goldstone particles used here are ($m_\pi = 140$ MeV, $m_K = 495$ MeV, and $m_\eta = 547$ MeV). The calculations are performed at the physical values of pion decay constant $f = 92.4$ MeV and of the coupling constants g and h that are extracted from the strong decay widths $g = 0.64 \pm 0.075$ and $h = 0.56 \pm 0.04$; for details, see [2]. The renormalization scale μ is chosen to be the average of the pion and kaon masses $\mu = 317$ MeV.

Name	J^P	Mass (MeV)	Name	J^P	Mass (MeV)	Name	J^P	Mass (MeV)
D^0	0^-	1864.84 ± 0.05	D^\pm	0^-	1869.61 ± 0.09	D_s^\pm	0^-	1968.30 ± 0.10
D^{*0}	1^-	2006.97 ± 0.08	$D^{*\pm}$	1^-	2010.27 ± 0.05	$D_s^{*\pm}$	1^-	2112.1 ± 0.4
D_0^0	0^+	2318 ± 29	D_0^\pm	0^+	...	$D_{s0}^{*\pm}$	0^+	2317.7 ± 0.6
$D_1^{0'}$	1^+	2427 ± 36	$D_1^{\pm'}$	1^+	...	$D_{s1}^{\pm'}$	1^+	2459.5 ± 0.6

TABLE I. The listed charm meson states have been used in our fitting. J^P is the angular momentum and parity of the meson. In our fitting, the masses of H_1 (H_1^*) are obtained by taking the isospin average of D^0 and D^\pm (D^{*0} and $D^{*\pm}$); for details please refer to the text. All masses are taken from the Particle Data Group [1] except the mass of the excited neutral nonstrange meson $D_1^{0'}$, which is reported by the BELLE collaboration [13].

The chiral-loop functions are fed with the difference of the physical masses of the charm mesons. Thus, the uniquely determined values of the parameters include contributions from terms beyond the loop order. Since these higher-order terms have not been considered in the chiral Lagrangian, their μ dependence cannot be canceled by existing coefficients. So, beta functions of the parameters are defined in order to estimate how much higher-order terms donate to the central values of those parameters. The resulting numerical values of the parameters which inhabit the odd-parity

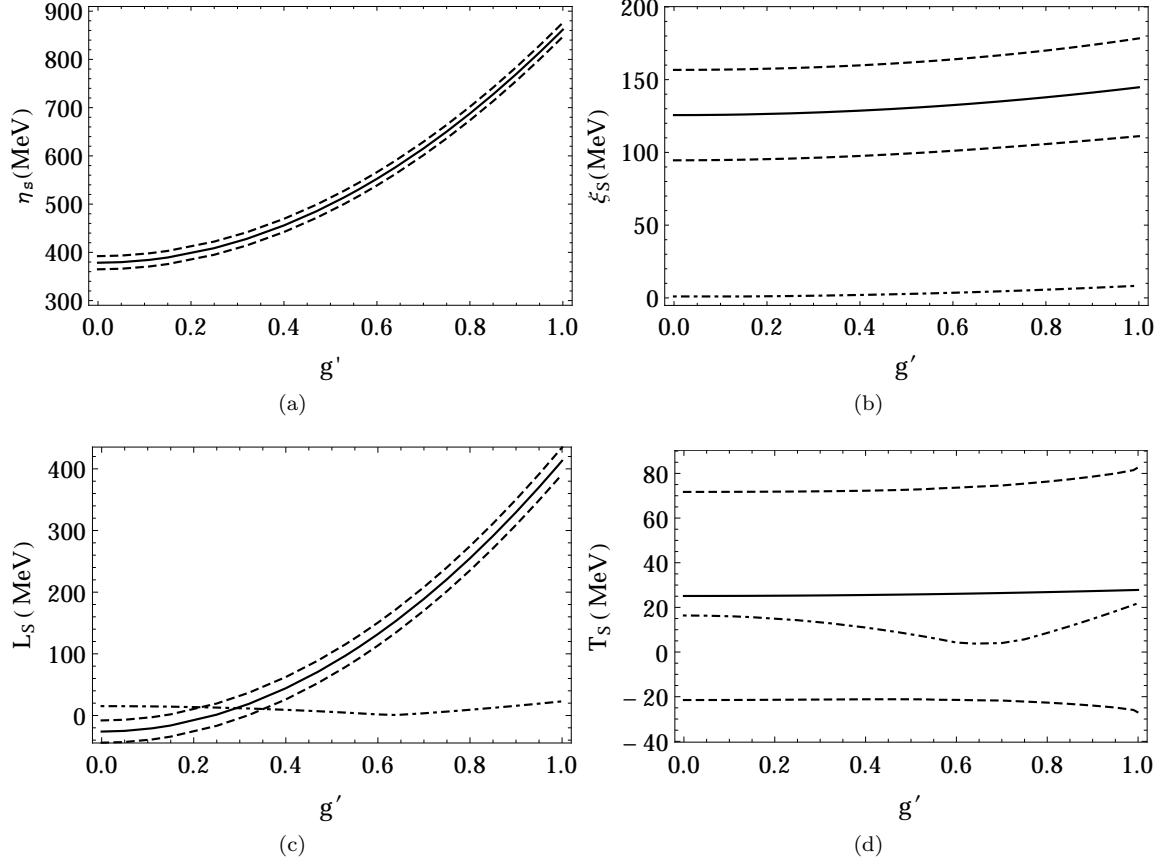


FIG. 2. Variation of (a) η_S , (b) ξ_S , (c) L_S , and (d) T_S with g' . The experimental uncertainties are shown by dashed lines surrounding the central values, and an estimate theoretical uncertainty is shown by dotted-dashed line. The theoretical uncertainty of the parameter η_S is a constant ± 5 MeV.

sector are

$$\begin{aligned} \eta_H &= 171.57 \pm 44 \pm 5 \text{ MeV}, \quad \xi_H = 150.95 \pm 5 \pm 5 \text{ MeV}, \\ L_H &= 242.71 \pm 40 \pm 18 \text{ MeV}, \quad T_H = -52.21 \pm 18 \pm 15 \text{ MeV}, \end{aligned} \quad (10)$$

where the first uncertainty is the experimental error associated with physical masses of charm mesons and the second uncertainty is the theoretical error that we have estimated from the β -functions.

The situation for the even-parity parameters is different because the coupling constant g' is not determined experimentally. Since the value of the odd-parity coupling constant g is 0.64, it is plausible to consider values for g' in the range 0 to 1. The correlations between g' and η_S , ξ_S , L_S , T_S are shown in Fig. 2. The plots also show the associated experimental and theoretical errors.

Experimental information is not sufficient to separate the combinations of the LECs into pieces that respect and break chiral symmetry, which limits their usefulness for applications to other observables. Lattice QCD calculations would be required to perform further separations of terms. For example, lattice results on the charm meson spectroscopy undertaken in Refs. [19, 20] can be used to disentangle chirally symmetric parameters $\delta_{H;S}$ and $\Delta_{H;S}$ from chiral breaking terms.

V. PREDICTION FOR THE SPECTRUM OF ODD- AND EVEN-PARITY BOTTOM MESONS

Using the results from charm mesons, one can predict the spectra of the B mesons. To this end, the hyperfine operators in the theory, i.e., the parameters $\xi_{H;S}$, $T_{H;S}$ that break heavy quark symmetry, will be rescaled to define the mass formula for the odd- and even-parity bottom mesons. The rescaling can be achieved by multiplying these operators by the ratio of the finite charm and bottom quark masses, $\frac{m_c}{m_b}$.

Mass Scheme	Charm quark mass (GeV)	Bottom quark mass (GeV)	$\frac{m_c}{m_b}$
$\overline{\text{MS}}$ [1]	1.275 ± 0.025	4.18 ± 0.03	0.305
Pole [1]	1.67 ± 0.07	4.78 ± 0.06	0.349
1 S [1]	4.66 ± 0.03	..
Kinetic [22]	1.077 ± 0.074	4.549 ± 0.049	0.237

TABLE II. The charm and bottom $\overline{\text{MS}}$ masses are evaluated at their own scale, i.e., $\overline{m}_c(\overline{m}_c)$ and $\overline{m}_b(\overline{m}_b)$. In Ref. [1], the $\overline{\text{MS}}$ values are converted to the pole scheme. The ratio of charm and bottom masses obtained from the pole mass is close to the ratio of the pseudoscalar charm and bottom mesons $\frac{m_D}{m_B} = 0.35$. In the kinetic mass scheme, the charm and bottom masses are evaluated at $\mu = 1 \text{ GeV}$ [22].

The masses of the charm and bottom quarks are not directly measured. Many theoretical and computational methods have been developed to extract their values; for a review, see Refs. [1, 21]. In Table II, we list the charm and bottom quark masses evaluated from different mass schemes. Clearly, the extracted masses of the charm and bottom quarks are not uniquely defined. The values depend on the definition of the mass scheme used. It is not clear which is the best definition for our purposes. However, as the $\overline{\text{MS}}$ definition has a small associated uncertainty, it is convenient to choose the ratio obtained from it and add an extra uncertainty, of the order $O(\Lambda_{\text{QCD}})$, to cover the spread of $\frac{m_c}{m_b}$ resulting from different mass schemes. Thus, the hyperfine operators in our theory can be rescaled by the factor $\frac{m_c}{m_b} = 0.305 \pm 0.05$. In terms of the rescaled parameters, the mass formulas for the bottom mesons up to one-loop corrections are

$$\begin{aligned}
m_{B_a} &= \eta_H - \frac{3}{4} \frac{m_c}{m_b} \xi_H + \frac{\alpha_a}{3} L_H + \frac{\beta_a}{2} \frac{m_c}{m_b} T_H + \Sigma_{B_a}, \\
m_{B_a^*} &= \eta_H + \frac{1}{4} \frac{m_c}{m_b} \xi_H + \frac{\alpha_a}{3} L_H + \frac{\beta_a^*}{2} \frac{m_c}{m_b} T_H + \Sigma_{B_a^*}, \\
m_{B_{a0}} &= \eta_S - \frac{3}{4} \frac{m_c}{m_b} \xi_S + \frac{\alpha_a}{3} L_S + \frac{\beta_a}{2} \frac{m_c}{m_b} T_S + \Sigma_{B_{a0}}, \\
m_{B_{a0}^*} &= \eta_S + \frac{1}{4} \frac{m_c}{m_b} \xi_S + \frac{\alpha_a}{3} L_S + \frac{\beta_a^*}{2} \frac{m_c}{m_b} T_S + \Sigma_{B_{a0}^*},
\end{aligned} \tag{11}$$

where the self-energy Σ_B is a function of the mass difference of the B mesons and the masses of the light pseudoscalar mesons π , η , and K .

To predict the masses of the bottom mesons, it is suitable to choose the ground state of the nonstrange B meson as the reference mass to get the following independent splittings $m_{B^*} - m_B$, $m_{B_s} - m_B$, $m_{B_s^*} - m_B$, $m_{B_0} - m_B$, $m_{B_{s0}} - m_B$, $m_{B_0^*} - m_B$, and $m_{B_{s0}^*} - m_B$ where the symbols B , B_s , B^* , B_s^* , B_0 , B_{s0} , B_0^* , B_{s0}^* represent the nonstrange pseudoscalar, strange pseudoscalar, nonstrange vector, strange vector, nonstrange scalar, strange scalar, nonstrange axial-vector and strange axial-vector, respectively. The loop functions depend on the mass differences, and so these independent splittings form nonlinear equations. We have used an iterative method to solve them starting from the tree-level masses. The numerical values of these mass splittings are shown in Figs. 3 and 4.

Our theoretical prediction for masses (splittings) of the odd-parity B mesons are in good agreement with the available experimental data. In the PDG [1], the splittings within odd-parity B mesons are

$$m_{B^*} - m_B = 45.38 \pm 0.30 \text{ MeV}, \tag{12}$$

$$m_{B^{*+}} - m_{B^+} = 45.0 \pm 0.4 \text{ MeV}, \tag{13}$$

$$m_{B_s} - m_B = 87.33 \pm 0.23 \text{ MeV}, \tag{14}$$

$$m_{B_s^*} - m_{B_s} = 48.6 \pm 2.41 \text{ MeV}. \tag{15}$$

The mass difference $m_{B_s^*} - m_B$ can be obtained from the above splittings as follows:

$$\begin{aligned}
m_{B_s^*} - m_B &= (m_{B_s^*} - m_{B_s}) + (m_{B_s} - m_B) \\
&= 135.93 \pm 2.42 \text{ MeV}.
\end{aligned} \tag{16}$$

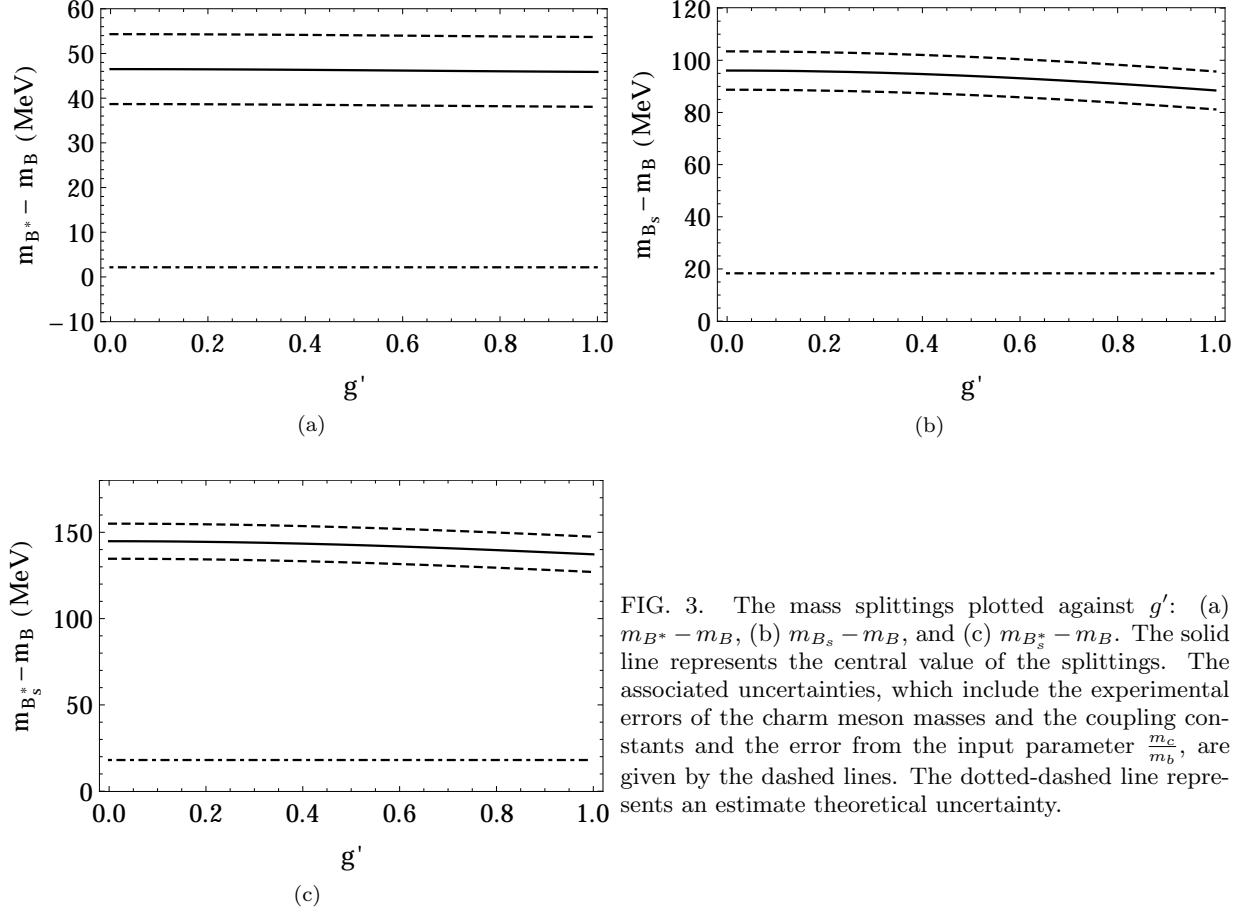


FIG. 3. The mass splittings plotted against g' : (a) $m_{B^*} - m_B$, (b) $m_{B_s} - m_B$, and (c) $m_{B_s^*} - m_B$. The solid line represents the central value of the splittings. The associated uncertainties, which include the experimental errors of the charm meson masses and the coupling constants and the error from the input parameter $\frac{m_c}{m_b}$, are given by the dashed lines. The dotted-dashed line represents an estimate theoretical uncertainty.

By comparing the results in Eq. (12) and Eq. (13) with the predicted splitting shown in Fig. 3(a), we find that the experimental measurement of hyperfine splitting of the nonstrange B mesons agrees with our theoretical prediction within 1σ standard deviation. Similarly, the measured mass difference $m_{B_s} - m_B$ [see Eq. (14)] agrees with our theoretical prediction [see Fig. 3(b)] within about 1σ standard deviation. Furthermore, the measured mass difference $m_{B_s^*} - m_B$ [see Eq. (16)] agrees with our theoretical prediction [see Fig. 3(c)] within 1σ standard deviation.

For the even-parity sector, the B -meson states have not yet been observed; thus, our results, which are shown in Fig. 4, provide useful information for experimentalists investigating such states.

For the predicted masses (splittings) of the even-parity sector, the strong dependence on the coupling g' is due to the large negative contribution from terms with

$$\frac{g'^2}{4f^2} n_f K_1(\omega, m) \simeq \frac{g'^2}{4f^2} n_f \left(-\frac{4}{16\pi^2} (\omega^2 - m^2) F(\omega, m) + \dots \right) \propto -\frac{g'^2}{f^2} n_f m^2 \sqrt{m^2 - \omega^2} \cos^{-1} \left(\frac{\omega}{m} \right) + \dots,$$

for $m^2 > \omega^2$ where $m = m_\eta, m_K$. The light-quark factor n_f is simply obtained from the Gell-Mann matrices, and its value reflects the number of independent self-energy loop diagrams which contribute to the process.

Before proceeding to comment on the $SU(3)$ -splittings within the predicted B -meson states, let us first briefly examine the charm meson masses given in Table I. Evidently, the strange and nonstrange splittings of the well determined states, i.e., $J^P = 0^-$ and $J^P = 1^-$, are consistent with the size of the $SU(3)$ breaking, $O(100 \text{ MeV})$. However, this is not the case for the even-parity sector where the central values of the splittings

$$m_{D_{s0}^{*\pm}} - m_{D_{s0}^{*0}} = -0.3 \pm 29 \text{ MeV}, \quad m_{D_{s1}^{\pm'}} - m_{D_0^{0'}} = 32.5 \pm 36 \text{ MeV}, \quad (17)$$

are inconsistent with the size of the $SU(3)$ breaking. The closeness of $m_{D_{s0}^{*\pm}}$ and $m_{D_0^{*0}}$ masses was the first observation of mass degeneracy in heavy-light mesons.

From the heavy quark symmetry, the observed mass degeneracy in the charm sector implies the similarity of m_{B_0} and $m_{B_{s0}}$ in the bottom sector. Our approach of using HHChPT shows that there is an accidental cancellation

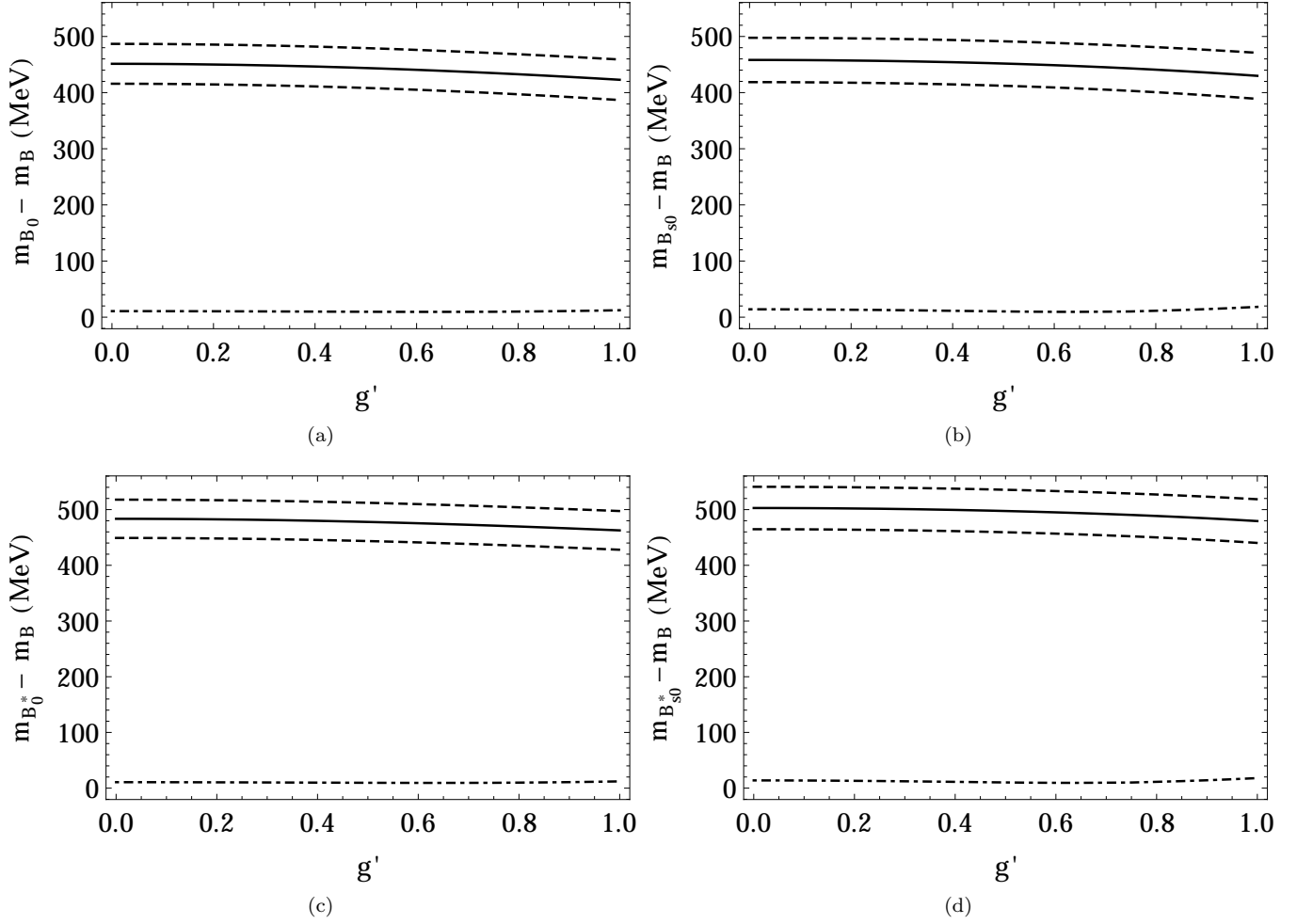


FIG. 4. The mass splittings plotted against g' : (a) $m_{B_0} - m_B$, (b) $m_{B_{s0}} - m_B$, (c) $m_{B_0^*} - m_B$, and (d) $m_{B_{s0}^*} - m_B$. The notation is the same as in Fig. 3.

between $SU(3)$ -breaking loop contributions and counterterms in the even-parity B -meson sector. Hence, it is obvious from Figs. 4(a) and 4(b) that the nonstrange and strange scalar bottom mesons are nearly degenerate, the difference between their central values is ~ 8 MeV. Moreover, the splitting between nonstrange and strange axial-vector bottom mesons is ~ 19 MeV; see Figs. 4(c) and 4(d). This result, which is inconsistent with the theoretical expectation on $SU(3)$ breaking, was observed in charm sector.

The difference between $SU(3)$ -splittings in the predicted B -meson sector is approximately equal to the ones in the observed D -meson sector times the rescaling factor, i.e.,

$$(m_{B_{s0}^*} - m_{B_0^*}) - (m_{B_{s0}} - m_{B_0}) \approx \frac{m_c}{m_b} \left[(m_{D_{s1}^{\pm'}} - m_{D_0^{0'}}) - (m_{D_{s0}^{\pm}} - m_{D_0^{*0}}) \right]. \quad (18)$$

This mass relation is consistent with the heavy quark spin-flavor symmetry.

It is worth mentioning that the work undertaken in Refs. [11, 23] was intended to investigate the closeness of nonstrange and strange scalars in the charm and bottom sectors, using, in addition to HHChPT, different potential models. They considered the hadronic loops effect to shift down the bare masses of scalar mesons. In their work, the hadronic loop contributions include only the coupling of D_{s0}^* to the lowest possible intermediate states, these states form members of $\frac{1}{2}^-$ -doublet in the notation of HHChPT. The self-energy contributions from the coupling of D_{s0}^* to the members of the $\frac{1}{2}^+$ -doublet have been neglected in Refs. [11, 23] which in turn indicates their analysis within HHChPT is incomplete. In Ref. [11], the authors concluded that the results of studying the mass degeneracy using HHChPT are not satisfactory, which is in fact not true as shown in Figs. 4(a) and 4(b).

Furthermore, the approach employed in Refs. [11, 23] of using bare masses in evaluating loop functions is inappropriate for the case of HHChPT. For example, the predicted masses of B_{s0}^* and B_0^* , as given in TABLE II in

Ref. [11], provide different splittings when using different bare masses in evaluating loop functions. More precisely, the mass difference $m_{B_{s_0}^*} - m_{B_0^*}$ is $\sim +100$ MeV when evaluating loop functions with bare masses given in Ref. [24] and is ~ -60 MeV when evaluating loop functions with bare masses taken from Ref. [25]. This shows that the loop integrals are sensitive to the input mass differences of the heavy mesons, so using bare masses is not appropriate. To avoid these problems, we use the self-consistently determined masses. As a result, there is an unavoidable theoretical uncertainty, which we estimate from higher-order contributions from the β function.

VI. SUMMARY

The aspects of mesons containing a single heavy quark are governed by the spin symmetry $SU(2)_s$ of the heavy quark and the chiral symmetry $SU(3)_L \times SU(3)_R$ of the light quarks. Incorporating both approximate symmetries in a single framework was achieved by defining the heavy hadron chiral perturbation theory. This effective theory was used to study the spectra and interactions of these heavy mesons. We studied the masses of the low-lying charm and bottom mesons using HHChPT. We expressed the masses of these heavy mesons up to third order, Q^3 , in the chiral expansion, where meson loops contribute. The heavy-hadron chiral Lagrangian has 12 unknown low-energy constants ($\delta_{H;S}$, $a_{H;S}$, $\sigma_{H;S}$, $\Delta_{H;S}$, $\Delta_{H;S}^{(a)}$, $\Delta_{H;S}^{(\sigma)}$) to describe eight measured masses of charm mesons. Hence, obtaining unique numerical values of the LECs is impossible. We used flavor and heavy quark symmetries to construct eight linear combinations ($\eta_{H;S}$, $\xi_{H;S}$, $L_{H;S}$, $T_{H;S}$) out of the LECs. By using this method, we reduced the number of unknown LECs to be comparable with the current experimental data on meson masses. Thus, one can express these parameters directly in terms of the physical masses and loop integrals. In contrast to previous approaches, we used physical meson masses in evaluating the heavy meson loops. As a result, the energy of any unstable particle is placed correctly relative to the decay threshold, and the imaginary part of the loop integral can be related to the experimental decay width. However, the resulting values for these parameters contain contributions beyond the order Q^3 of heavy-hadron chiral Lagrangian. This is due to using empirical masses which generate higher order μ -dependent terms that cannot be renormalized using μ -dependent counterterms of our Lagrangian. To this end, we chose to define the β functions for these parameters to estimate the contributions from higher-order terms. Having fitted the linear combinations of the LECs to the D -meson spectrum, we rescale the hyperfine combinations to predict the masses of odd- and even-parity bottom mesons. In our calculations, we used a self-consistent approach to extract the B -meson masses; i.e., the values we started with to evaluate the mass splittings within B -meson states are the same as the resultant mass splittings. The predicted masses from our theory are in good agreement with experimentally measured masses for the case of the odd-parity sector. For the even-parity sector, the B -meson states have not yet been observed; thus, our results provide useful information for experimentalists investigating such states.

The approach developed in this paper can be extended to predict the spectra of the other doublet of the P -wave states, i.e., $S^p = \frac{3}{2}^+$, where S is the total angular momentum of the light degrees of freedom, and p is the parity. The spin-parity quantum numbers of these states are 1^+ and 2^+ . This requires introducing a new (tensor) field to describe the dynamics of these states in the chiral Lagrangian. The general structure of the relevant chiral Lagrangian with tensor fields is represented in [2, 6, 7] for instance.

ACKNOWLEDGMENTS

I am grateful to Michael C. Birse, whose guidance and support helped me to develop an understanding of the subject.

Appendix A: Self-Energies of Charm Mesons

The explicit expressions for the self-energies of the charm mesons are

$$\begin{aligned} \Sigma_{H_1} = & \frac{g^2}{4f^2} \left[3K_1(m_{H_1^*} - m_{H_1}, m_\pi) + \frac{1}{3}K_1(m_{H_1^*} - m_{H_1}, m_\eta) + 2K_1(m_{H_3^*} - m_{H_1}, m_K) \right] \\ & + \frac{h^2}{4f^2} \left[3K_2(m_{S_1} - m_{H_1}, m_\pi) + \frac{1}{3}K_2(m_{S_1} - m_{H_1}, m_\eta) + 2K_2(m_{S_3} - m_{H_1}, m_K) \right], \end{aligned} \quad (\text{A1})$$

$$\begin{aligned}
\Sigma_{H_1^*} = & \frac{g^2}{4f^2} \left[K_1(m_{H_1} - m_{H_1^*}, m_\pi) + \frac{1}{9} K_1(m_{H_1} - m_{H_1^*}, m_\eta) + \frac{2}{3} K_1(m_{H_3} - m_{H_1^*}, m_K) \right] \\
& + \frac{g^2}{4f^2} \left[2K_1(0, m_\pi) + \frac{2}{9} K_1(0, m_\eta) + \frac{4}{3} K_1(m_{H_3^*} - m_{H_1^*}, m_K) \right] \\
& + \frac{h^2}{4f^2} \left[3K_2(m_{S_1^*} - m_{H_1^*}, m_\pi) + \frac{1}{3} K_2(m_{S_1^*} - m_{H_1^*}, m_\eta) + 2K_2(m_{S_3^*} - m_{H_1^*}, m_K) \right],
\end{aligned} \tag{A2}$$

$$\begin{aligned}
\Sigma_{H_3} = & \frac{g^2}{4f^2} \left[\frac{4}{3} K_1(m_{H_3^*} - m_{H_3}, m_\eta) + 4K_1(m_{H_1^*} - m_{H_3}, m_K) \right] \\
& + \frac{h^2}{4f^2} \left[\frac{4}{3} K_2(m_{S_3} - m_{H_3}, m_\eta) + 4K_2(m_{S_1} - m_{H_3}, m_K) \right],
\end{aligned} \tag{A3}$$

$$\begin{aligned}
\Sigma_{H_3^*} = & \frac{g^2}{4f^2} \left[\frac{4}{9} K_1(m_{H_3} - m_{H_3^*}, m_\eta) + \frac{4}{3} K_1(m_{H_1} - m_{H_3^*}, m_K) \right] \\
& + \frac{g^2}{4f^2} \left[\frac{8}{9} K_1(0, m_\eta) + \frac{8}{3} K_1(m_{H_1^*} - m_{H_3^*}, m_K) \right] \\
& + \frac{h^2}{4f^2} \left[\frac{4}{3} K_2(m_{S_3^*} - m_{H_3^*}, m_\eta) + 4K_2(m_{S_1^*} - m_{H_3^*}, m_K) \right],
\end{aligned} \tag{A4}$$

$$\begin{aligned}
\Sigma_{S_1} = & \frac{g'^2}{4f^2} \left[3K_1(m_{S_1^*} - m_{S_1}, m_\pi) + \frac{1}{3} K_1(m_{S_1^*} - m_{S_1}, m_\eta) + 2K_1(m_{S_3^*} - m_{S_1}, m_K) \right] \\
& + \frac{h^2}{4f^2} \left[3K_2(m_{H_1} - m_{S_1}, m_\pi) + \frac{1}{3} K_2(m_{H_1} - m_{S_1}, m_\eta) + 2K_2(m_{H_3} - m_{S_1}, m_K) \right],
\end{aligned} \tag{A5}$$

$$\begin{aligned}
\Sigma_{S_1^*} = & \frac{g'^2}{4f^2} \left[K_1(m_{S_1} - m_{S_1^*}, m_\pi) + \frac{1}{9} K_1(m_{S_1} - m_{S_1^*}, m_\eta) + \frac{2}{3} K_1(m_{S_3} - m_{S_1^*}, m_K) \right] \\
& + \frac{g'^2}{4f^2} \left[2K_1(0, m_\pi) + \frac{2}{9} K_1(0, m_\eta) + \frac{4}{3} K_1(m_{S_3^*} - m_{S_1^*}, m_K) \right] \\
& + \frac{h^2}{4f^2} \left[3K_2(m_{H_1^*} - m_{S_1^*}, m_\pi) + \frac{1}{3} K_2(m_{H_1^*} - m_{S_1^*}, m_\eta) + 2K_2(m_{H_3^*} - m_{S_1^*}, m_K) \right],
\end{aligned} \tag{A6}$$

$$\begin{aligned}
\Sigma_{S_3} = & \frac{g'^2}{4f^2} \left[\frac{4}{3} K_1(m_{S_3^*} - m_{S_3}, m_\eta) + 4K_1(m_{S_1^*} - m_{S_3}, m_K) \right] \\
& + \frac{h^2}{4f^2} \left[\frac{4}{3} K_2(m_{H_3} - m_{S_3}, m_\eta) + 4K_2(m_{H_1} - m_{S_3}, m_K) \right],
\end{aligned} \tag{A7}$$

$$\begin{aligned}
\Sigma_{S_3^*} = & \frac{g'^2}{4f^2} \left[\frac{4}{9} K_1(m_{S_3} - m_{S_3^*}, m_\eta) + \frac{4}{3} K_1(m_{S_1} - m_{S_3^*}, m_K) \right] \\
& + \frac{g'^2}{4f^2} \left[\frac{8}{9} K_1(0, m_\eta) + \frac{8}{3} K_1(m_{S_1^*} - m_{S_3^*}, m_K) \right] \\
& + \frac{h^2}{4f^2} \left[\frac{4}{3} K_2(m_{H_3^*} - m_{S_3^*}, m_\eta) + 4K_2(m_{H_1^*} - m_{S_3^*}, m_K) \right].
\end{aligned} \tag{A8}$$

The chiral loop integrals are

$$\begin{aligned} K_1(\omega, m) &= \frac{1}{16\pi^2} \left[(-2\omega^3 + 3m^2\omega) \ln \left(\frac{m^2}{\mu^2} \right) - 4(\omega^2 - m^2)F(\omega, m) + \frac{16}{3}\omega^3 - 7\omega m^2 \right], \\ K_2(\omega, m) &= \frac{1}{16\pi^2} \left[(-2\omega^3 + m^2\omega) \ln \left(\frac{m^2}{\mu^2} \right) - 4\omega^2 F(\omega, m) + 4\omega^3 - \omega m^2 \right], \end{aligned} \quad (\text{A9})$$

renormalized in the $\overline{\text{MS}}$ scheme. The function $F(\omega, m)$ is given by

$$F(\omega, m) = \begin{cases} -\sqrt{m^2 - \omega^2} \cos^{-1}(\frac{\omega}{m}), & m^2 > \omega^2, \\ \sqrt{\omega^2 - m^2} [i\pi - \cosh^{-1}(-\frac{\omega}{m})], & \omega < -m, \\ \sqrt{\omega^2 - m^2} \cosh^{-1}(\frac{\omega}{m}), & \omega > m. \end{cases} \quad (\text{A10})$$

It is worth mentioning that the expression for $K_1(\omega, m)$ in Ref. [9] does not agree with our expression. Some finite pieces are missed due to the inconsistent use of dimensional regularization; i.e., the authors set $d = 4$ before expanding in powers of $4 - d$. However, our calculation when using the chiral function $K_1(\omega, m)$ from Ref. [9], i.e.,

$$K_1(\omega, m) = \frac{1}{16\pi^2} \left[(-2\omega^3 + 3m^2\omega) \ln \left(\frac{m^2}{\mu^2} \right) - 4(\omega^2 - m^2)F(\omega, m) + 4\omega^3 - 5\omega m^2 \right], \quad (\text{A11})$$

does not affect much the results on the B meson spectra. The difference between the obtained results using our expression and the ones in Ref. [9] is less than 1 MeV. However, the values of parameters that break flavor and/or spin symmetries, i.e., $\xi_{H;S}$, $L_{H;S}$, $T_{H;S}$, are much affected. For instance, the central values of odd-parity parameters given in Eq. (10) become

$$\eta_H = 171.57 \text{ MeV}, \quad \xi_H = 173.04 \text{ MeV}, \quad L_H = 263.13 \text{ MeV}, \quad T_H = -29.54 \text{ MeV}. \quad (\text{A12})$$

Our expression for $K_2(\omega, m)$ agrees with the expression presented in Ref. [9]; for details, see Appendix B.

Appendix B: Calculation of Loop Corrections

For the sake of simplicity, we restrict our discussion to $SU(2)$ HHChPT with nonstrange D mesons. Our calculations of loop diagrams differ from those in Refs. [7, 9, 26] in two aspects:

- i) Dimensional regularization is used consistently.
- ii) To maintain the heavy quark symmetry at the quantum loop level, the nonrelativistic heavy meson fields are defined in four dimensions.

In Figs. 5 and 6, we show the Feynman diagrams of the one-loop correction to the masses of D mesons. In evaluating loop integrals for these diagrams, one has to be careful with the tensor structure to get the correct expressions. For this purpose, we will calculate loop integrals for diagrams $a - e$ in Fig. 5. The results hold for diagrams with a similar tensor structure of even-parity sector as shown in Fig. 6.

Let us start with the loop diagram a in Fig. 5, which contributes to the self-energy of the H_1 field, i.e., the D^+

$$\begin{aligned} i\Sigma_{H_1}^{(a)} &= 3 \left(\frac{g}{2f} \right)^2 \mu^{4-d} \int \frac{d^d q}{(2\pi)^d} \frac{q^\mu q^\nu (g_{\mu\nu} - v_\mu v_\nu)}{(q \cdot v - \omega_a + i\epsilon)(q^2 - m_\pi^2 + i\epsilon)} \\ &= 3 \left(\frac{g}{2f} \right)^2 (g_{\mu\nu} - v_\mu v_\nu) \mu^{4-d} \int \frac{d^d q}{(2\pi)^d} \frac{q^\mu q^\nu}{(q \cdot v - \omega_a + i\epsilon)(q^2 - m_\pi^2 + i\epsilon)}, \end{aligned} \quad (\text{B1})$$

where ω is the mass difference between internal and external heavy meson states. The factor 3 results from Pauli matrices $(\tau_i^2)_{\alpha\beta} = 3\delta_{\alpha\beta}$, where for one-loop diagrams in which a single pion is exchanged $\alpha = \beta$, so $\delta_{\alpha\alpha} = 1$.

The chiral loop integral is divergent. However, there are many ways to regulate the above loop-integral and each one introduces a new momentum scale of which physical observables must be independent. In field theory, the so-called dimensional regularization scheme (DR) is widely used since it preserves gauge and chiral symmetries as well as Lorentz (Galilean) invariance for relativistic (nonrelativistic) systems.

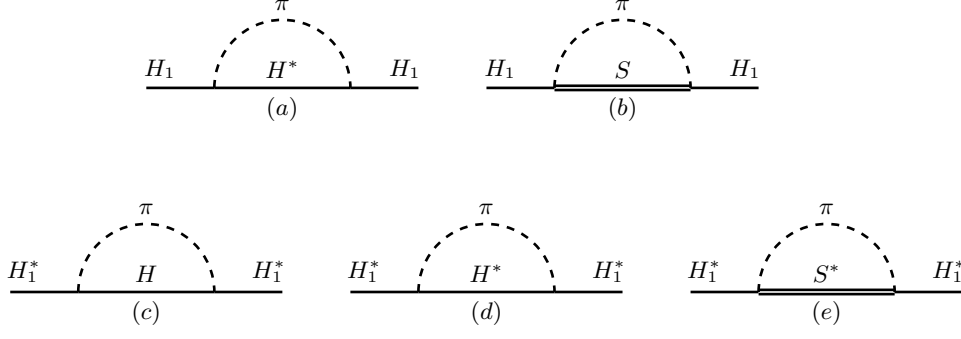


FIG. 5. Feynman diagrams shown in (a) and (b) represent the self-energy of the H_1 field and those shown in (c)-(e) represent the self-energy of the H_1^* field.

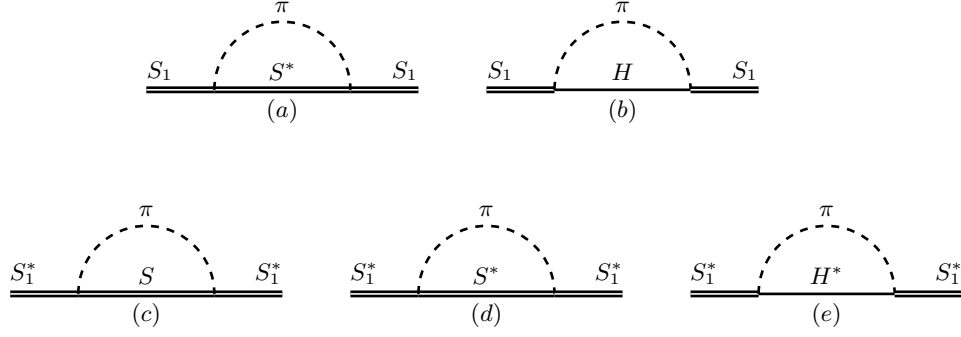


FIG. 6. Feynman diagrams shown in (a) and (b) represent the self-energy of the S_1 field and those shown in (c)-(e) represent the self-energy of the S_1^* field.

For loop integrals containing two or more powers of q (momentum of the internal pion) in the numerator, the standard procedure of evaluating them is to break them up into simple integrals that can then be easily calculated [12, 27]. Thus, one can write

$$i\mu^{4-d} \int \frac{d^d q}{(2\pi)^d} \frac{q^\mu q^\nu}{(q \cdot v - \omega + i\epsilon)(q^2 - m_\pi^2 + i\epsilon)} = g^{\mu\nu} J_2 + v^\mu v^\nu J_3, \quad (\text{B2})$$

where

$$J_2 = \frac{1}{d-1} [(m_\pi^2 - \omega^2) J_0 - \omega J_\pi], \quad (\text{B3})$$

and

$$J_3 = \frac{1}{d-1} [(d\omega^2 - m_\pi^2) J_0 + \omega d J_\pi]. \quad (\text{B4})$$

The explicit expression for J_0 is

$$\begin{aligned} J_0 &= i\mu^{4-d} \int \frac{d^d q}{(2\pi)^d} \frac{1}{(q \cdot v - \omega + i\epsilon)(q^2 - m_\pi^2 + i\epsilon)} \\ &= \frac{\omega}{8\pi^2} [1 + \text{R} - \ln(\frac{m_\pi^2}{\mu^2}) - \frac{2}{\omega} F(\omega, m_\pi)], \end{aligned}$$

and the expression for J_π is

$$J_\pi = i\mu^{4-d} \int \frac{d^d q}{(2\pi)^d} \frac{1}{(q^2 - m_\pi^2 + i\epsilon)} = \frac{m_\pi^2}{16\pi^2} [\ln(\frac{m_\pi^2}{\mu^2}) - \text{R}],$$

where $R = \frac{2}{4-d} - \gamma_E + \ln(4\pi) + 1$ contains a pole at $d = 4$. In these expressions, μ is the renormalization scale. The function $F(\omega, m_\pi)$ is given in Eq. (A10).

To use dimensional regularization consistently, one has to set $d = 4$ after expanding J_2 and J_3 to first order in $4 - d$. If one sets $d = 4$ before expanding in powers of $4 - d$ as in Refs. [7, 26], the expressions for J_2 and J_3 will be missing some finite pieces where $\frac{1}{d-1}R = \frac{1}{3}R + \frac{2}{9} \neq \frac{1}{3}R$. If there is only one integral, then the different constants can be absorbed by different renormalization schemes; i.e., this corresponds to some modified subtraction schemes. For the case of two integrals with different finite terms, there is no single consistent renormalization scheme; i.e., the differences cannot be hidden in renormalization schemes.

By expanding Eqs. (B3) and (B4) to first order in $4 - d$ and then taking $d = 4$, we get

$$J_2 = \frac{1}{16\pi^2} \left[\left(\frac{2}{3}\omega^3 - m_\pi^2\omega \right) \ln\left(\frac{m_\pi^2}{\mu^2}\right) + \frac{4}{3}(\omega^2 - m_\pi^2)F(\omega, m_\pi) - \frac{2}{3}\omega^3\left(R + \frac{5}{3}\right) + \frac{1}{3}\omega m_\pi^2(3R + 4) \right], \quad (\text{B5})$$

and

$$J_3 = \frac{1}{16\pi^2} \left[(2m_\pi^2\omega - \frac{8}{3}\omega^3) \ln\left(\frac{m_\pi^2}{\mu^2}\right) - \frac{4}{3}(4\omega^2 - m_\pi^2)F(\omega, m_\pi) + \frac{8}{3}\omega^3\left(R + \frac{7}{6}\right) - \frac{2}{3}\omega m_\pi^2(3R + 2) \right]. \quad (\text{B6})$$

Now, by substituting Eq. (B2) into Eq. (B1), one gets

$$\begin{aligned} i\Sigma_{H_1}^{(a)} &= 3 \left(\frac{g}{2f} \right)^2 (g_{\mu\nu} - v_\mu v_\nu) (-i(g^{\mu\nu}J_2 + v^\mu v^\nu J_3)) \\ &= 3i \left(\frac{g}{2f} \right)^2 (1 - g_{\mu\nu}g^{\mu\nu})J_2. \end{aligned} \quad (\text{B7})$$

As we have chosen to define the heavy meson fields in four dimensions, the contraction of the metric tensors is $g_{\mu\nu}g^{\mu\nu} = 4$. This is quite different from regularizing gauge theories in which the components of the gauge boson fields are continued in d dimensions to maintain the gauge invariance. In contrast, here it is important that regularization keeps the integrals of Figs. 5(a), 5(c), and 5(d) equal. Our purpose is to preserve the heavy quark symmetry. As will be shown below, our choice of defining the meson field as four dimensional maintains this.

Thus, Eq. (B7) becomes

$$i\Sigma_{H_1}^{(a)} = 3i \left(\frac{g}{2f} \right)^2 (-3J_2) = 3i \left(\frac{g}{2f} \right)^2 K_1(\omega_a, m_\pi), \quad (\text{B8})$$

where in the last step we introduced the chiral function $K_1(\omega, m_\pi)$. This can be related to J_2 as

$$\begin{aligned} K_1(\omega, m_\pi) &= -3J_2 = -\frac{3}{d-1}[(m_\pi^2 - \omega^2)J_0 - \omega J_\pi] \\ &= \frac{1}{16\pi^2} \left[(-2\omega^3 + 3m_\pi^2\omega) \ln\left(\frac{m_\pi^2}{\mu^2}\right) - 4(\omega^2 - m_\pi^2)F(\omega, m_\pi) + 2\omega^3\left(R + \frac{5}{3}\right) - \omega m_\pi^2(3R + 4) \right], \end{aligned} \quad (\text{B9})$$

where this represents the contribution to self-energy of charm mesons from one-loop diagrams with interacting particles belonging to the same doublets.

Now, we want to calculate the integral of the loop diagram in Fig. 5(c), which contributes to the self-energy of the

vector charm meson

$$\begin{aligned}
i \Sigma_{H_1^*}^{(c)} &= 3 \left(\frac{g}{2f} \right)^2 \left(-\mu^{4-d} \int \frac{d^d q}{(2\pi)^d} \frac{\epsilon \cdot q \epsilon \cdot q}{(q \cdot v - \omega_c + i\epsilon)(q^2 - m_\pi^2 + i\epsilon)} \right) \\
&= 3 \left(\frac{g}{2f} \right)^2 \left(-\epsilon_\mu^* \epsilon_\nu \mu^{4-d} \int \frac{d^d q}{(2\pi)^d} \frac{q^\mu q^\nu}{(q \cdot v - \omega_c + i\epsilon)(q^2 - m_\pi^2 + i\epsilon)} \right) \\
&= 3i \left(\frac{g}{2f} \right)^2 \epsilon_\mu^* \epsilon_\nu (g^{\mu\nu} J_2 + v^\mu v^\nu J_3),
\end{aligned} \tag{B10}$$

where the last line is obtained by using Eq. (B2). Since $v_\mu \epsilon^\mu = 0$ and $\epsilon_\mu^* \epsilon^\mu = -1$, $\Sigma_{H_1^*}^{(c)}$ is

$$i \Sigma_{H_1^*}^{(c)} = -3i \left(\frac{g}{2f} \right)^2 J_2 = i \left(\frac{g}{2f} \right)^2 K_1(\omega_c, m_\pi). \tag{B11}$$

The integral of one-loop diagram in Fig. 5(d), which contributes to the self-energy of the vector charm meson, is

$$\begin{aligned}
i \Sigma_{H_1^*}^{(d)} &= 3 \left(\frac{g}{2f} \right)^2 \left(-\mu^{4-d} \int \frac{d^d q}{(2\pi)^d} \frac{\epsilon^{\mu' \nu' \rho' \sigma'} \epsilon_{\mu'}^* v_{\nu'} q_{\rho'} (g_{\sigma \sigma'} - v_{\sigma'} v_\sigma) \epsilon^{\mu \nu \rho \sigma} \epsilon_\mu v_\nu q_\rho}{(q \cdot v - \omega_d + i\epsilon)(q^2 - m_\pi^2 + i\epsilon)} \right) \\
&= -3i \left(\frac{g}{2f} \right)^2 \epsilon^{\mu' \nu' \rho' \sigma'} \epsilon_{\mu' \nu' \rho' \sigma'} \epsilon_\mu^* \epsilon^\mu v_{\nu'} v^{\nu'} J_2.
\end{aligned} \tag{B12}$$

As $v \cdot v = 1$, $\epsilon \cdot v = 0$, and $\epsilon \cdot \epsilon = -1$, the contraction between indices of the totally antisymmetric tensors yields $-2!$. Thus, $\Sigma_{H_1^*}^{(d)}$ becomes

$$i \Sigma_{H_1^*}^{(d)} = 3i \left(\frac{g}{2f} \right)^2 (-2J_2) = 2i \left(\frac{g}{2f} \right)^2 K_1(\omega_d, m_\pi). \tag{B13}$$

Clearly, our choice of defining meson fields in four dimensions, which gives $g_{\mu\nu} g^{\mu\nu} = 4$ for the loop integral of Fig. 5(a), yields results equal to the loop integrals of Figs. 5(c) and 5(d). The results of the diagrams in Figs. 6(a), 6(c), and 6(d) are similar to the ones of Figs. 5(a), 5(c), and 5(d), respectively.

Now, we evaluate the loop integrals for graphs describing the interaction of heavy mesons with opposite parity. To this end, let us begin with the second one-loop contribution to self-energy of H_1 which is shown in Fig. 5(b)

$$\begin{aligned}
i \Sigma_{H_1}^{(b)} &= 3 \left(\frac{h}{2f} \right)^2 \left(-\mu^{4-d} \int \frac{d^d q}{(2\pi)^d} \frac{v \cdot q v \cdot q}{(q \cdot v - \omega_b + i\epsilon)(q^2 - m_\pi^2 + i\epsilon)} \right) \\
&= 3 \left(\frac{h}{2f} \right)^2 \left(-v_\mu v_\nu \mu^{4-d} \int \frac{d^d q}{(2\pi)^d} \frac{q^\mu q^\nu}{(q \cdot v - \omega_b + i\epsilon)(q^2 - m_\pi^2 + i\epsilon)} \right).
\end{aligned} \tag{B14}$$

Similarly, substituting Eq. (B2) into Eq. (B14) gives

$$\begin{aligned}
i \Sigma_{H_1}^{(b)} &= 3i \left(\frac{h}{2f} \right)^2 v_\mu v_\nu (g^{\mu\nu} J_2 + v^\mu v^\nu J_3) \\
&= 3i \left(\frac{h}{2f} \right)^2 (J_2 + J_3) = 3i \left(\frac{h}{2f} \right)^2 K_2(\omega_b, m_\pi),
\end{aligned} \tag{B15}$$

where

$$\begin{aligned}
K_2(\omega, m_\pi) &= J_2 + J_3 = \omega^2 J_0 + \omega J_\pi = \frac{1}{16\pi^2} [(-2\omega^3 + m_\pi^2 \omega) \ln\left(\frac{m_\pi^2}{\mu^2}\right) - 4\omega^2 F(\omega, m_\pi) \\
&\quad + 2\omega^3(1 + R) - \omega m_\pi^2 R].
\end{aligned} \tag{B16}$$

For the one-loop diagram with (heavy) interacting particles belonging to different doublets, the contribution to the self-energy is given by the chiral function $K_2(\omega, m_\pi)$.

The integral of the one-loop diagram shown in Fig. 5(e), which contributes to the self-energy of the vector meson, is

$$\begin{aligned}
 i\Sigma_{H_1^*}^{(e)} &= 3 \left(\frac{h}{2f} \right)^2 \mu^{4-d} \int \frac{d^d q}{(2\pi)^d} \frac{\epsilon_\mu^* v \cdot q (g^{\mu\nu} - v^\mu v^\nu) v \cdot q \epsilon_\nu}{(q \cdot v - \omega_e + i\epsilon)(q^2 - m_\pi^2 + i\epsilon)} \\
 &= 3 \left(\frac{h}{2f} \right)^2 \epsilon_\mu^* \epsilon_\nu (g^{\mu\nu} - v^\mu v^\nu) v_\alpha v_\beta \mu^{4-d} \int \frac{d^d q}{(2\pi)^d} \frac{q^\alpha q^\beta}{(q \cdot v - \omega_e + i\epsilon)(q^2 - m_\pi^2 + i\epsilon)} \\
 &= -3 \left(\frac{h}{2f} \right)^2 v_\alpha v_\beta \mu^{4-d} \int \frac{d^d q}{(2\pi)^d} \frac{q^\alpha q^\beta}{(q \cdot v - \omega_e + i\epsilon)(q^2 - m_\pi^2 + i\epsilon)}.
 \end{aligned} \tag{B17}$$

Similarly, substituting Eq. (B2) into Eq. (B17) gives

$$\begin{aligned}
 i\Sigma_{H_1^*}^{(e)} &= 3i \left(\frac{h}{2f} \right)^2 v_\alpha v_\beta (g^{\alpha\beta} J_2 + v^\alpha v^\beta J_3) = 3i \left(\frac{h}{2f} \right)^2 (J_2 + J_3) \\
 &= 3i \left(\frac{h}{2f} \right)^2 K_2(\omega_e, m_\pi).
 \end{aligned} \tag{B18}$$

The loop integrals of the diagrams in Figs. 6(b) and 6(e) are similar to the result of Figs. 5(b) and 5(e), respectively.

-
- [1] K.A. Olive *et al.* (Particle Data Group Collaboration), Chin. Phys. C, **38**, 090001 (2014) and 2015 update [<http://pdg.lbl.gov/>].
 - [2] P. Colangelo, F. De Fazio, F. Giannuzzi and S. Nicotri, Phys. Rev. D **86**, 054024 (2012).
 - [3] M. Wise, Phys. Rev. D **45**, R2188 (1992).
 - [4] E. Jenkins, Nucl. Phys. B **412**, 181 (1994).
 - [5] P. L. Cho, Nucl. Phys. B **396**, 183 (1993) [Erratum-ibid. B **421**, 683 (1994)].
 - [6] A. F. Falk and M. E. Luke, Phys. Lett. B **292**, 119 (1992).
 - [7] R. Casalbuoni *et al.*, Phys. Rep. **281**, 145 (1997).
 - [8] X. W. Kang, B. Kubis, C. Hanhart and Ulf-G. Meissner, Phys. Rev. D **89**, 053015 (2014).
 - [9] T. Mehen and R. Springer, Phys. Rev. D **72**, 034006 (2005).
 - [10] B. Ananthanarayana, S. Banerjee, K. Shivaraja and A. Upadhyaya, Phys. Lett. B **651**, 124 (2007).
 - [11] H.Y. Cheng and F.S. Yu, Phys. Rev. D **89**, 114017, (2014).
 - [12] S. Scherer, Adv. Nucl. Phys. **27**, 277 (2003).
 - [13] K. Abe *et al.* (BELLE Collaboration), Phys. Rev. D **69**, 112002 (2004).
 - [14] S. K. Choi *et al.* (BELLE Collaboration), Phys. Rev. Lett. **91**, 262001 (2003).
 - [15] S. Anderson *et al.* (CLEO Collaboration), Nucl. Phys. **A663**, 647 (2000).
 - [16] D. Besson *et al.* (CLEO Collaboration), Phys. Rev. D **68**, 032002 (2003).
 - [17] J. M. Link *et al.* (FOCUS Collaboration), Phys. Lett. B **586**, 11 (2004).
 - [18] B. Aubert, *et al.* (BABAR Collaboration), Phys. Rev. Lett. **90** 242001 (2003).
 - [19] S. AOKI *et al.* (PACS-CS Collaboration), Phys. Rev. D **79**, 034503 (2009).
 - [20] D. Mohler and R. M. Woloshyn, Phys. Rev. D **84**, 054505 (2011).
 - [21] I. Bigi, M. Shifman, and N. Uraltsev, Ann. Rev. Nucl. Part. Sci. **47**, 591 (1997).
 - [22] B. Aubert *et al.* (BABAR Collaboration), Phys. Rev. D **81**, 032003 (2010).
 - [23] Feng-Kun Guo, Siegfried Krewald, and Ulf-G. Meissner, Phys. Lett. B **665** 157 (2008).
 - [24] M. Di Pierro and E. Eichten, Phys. Rev. D **64**, 114004 (2001).
 - [25] S. Godfrey and R. Kokoski, Phys. Rev. D **43**, 1679 (1991).
 - [26] C. G. Boyd and B. Grinstein, Nucl. Phys. B **442**, 205 (1995).
 - [27] V. Bernard, N. Kaiser, and Ulf-G. Meissner, Int. J. Mod. Phys. E **4**, 193 (1995).